Solution and Surface Charge Properties of Shell Cross-Linked Knedel Nanoparticles

Edward E. Remsen,*,† K. Bruce Thurmond II,† and Karen L. Wooley‡

Monsanto Company, 800 North Lindbergh Boulevard, St. Louis, Missouri 63167, and Department of Chemistry, Washington University, One Brookings Drive, St. Louis, Missouri 63130

Received December 18, 1998; Revised Manuscript Received April 6, 1999

ABSTRACT: Solution-state characterizations of poly(4-vinylpyridine):polystyrene (PVP:PS) shell cross-linked knedel nanoparticles (SCK's) are described. A combination of techniques, including dynamic light scattering, electrophoretic light scattering, and analytical ultracentrifugation, are used to determine the hydrodynamic diameter, surface charge characteristics, molecular weight, and aggregation number of the SCK's and their micelle precursors. The use of analytical ultracentrifugation is highlighted because of the wealth of information it provides in characterizing SCK solution behavior. The analysis of SCK's indicates that particle diameter, molecular weight, and aggregation increase with increasing PS chain length of the PVP:PS block copolymer used to prepare the SCK. Measurements of electrophoretic mobility and zeta potential via electrophoretic light scattering point to partial burial of charge below the particle surface of quaternized PVP units comprising the shell of the SCK. By contrast, the characterization of corresponding solution properties for the non-cross-linked micelle precursors is problematic due to significant particle heterogeneity and nonideal solution behavior. The comparison of solution data for SCK's and micelle precursors clearly indicates stabilization of SCK particles is achieved through shell cross-linking.

Introduction

The creation of novel nanomaterials with the appropriate size and function to potentially find application in nanotechnological devices or as biomimics in biotechnology is an active and highly promising area of research.[1−5] Methods for the production of nanomaterials are being actively pursued by researchers across disciplinary boundaries.[6−12] One of the greatest challenges involved in the development of nanoscale objects is accurate characterization of the composition, size, structure, and properties. This challenge must be met in order to advance nanoscience into nanotechnology.

Shell cross-linked knedel-like (SCK) nanospheres have been recently reported as unique nanometer-sized spheres with an amphiphilic core−shell morphology.[13] SCK's are prepared by intramicellar cross-linking of polymer chains located within the shell domain of polymer micelles. Therefore, these structures have been proposed as dimensionally stable polymer micelles, which will possess unique behavior and expand the realm of potential uses of micellar assemblies ranging from biomimetic gene therapy agents to fillers for engineering composites. However, thorough examination of the aqueous solution-state properties of such nanoscale micellar particles composed of a cross-linked network shell layer surrounding a non-cross-linked hydrophobic domain was not previously made. Herein, we report the characterization of solution-state properties of SCK's and polymer micelles by dynamic light scattering (DLS), electrophoretic light scattering (ELS), and analytical ultracentrifugation (AU). The use of multiple characterization techniques provides a more complete picture of the thermodynamic and hydrodynamic properties of these self-associating polymers. The use of analytical ultracentrifugation is highlighted in this study. AU has traditionally been a favored characterization tool for protein solution properties analysis.[14] The commercial availability of a new generation of AU instrumentation, with enhanced capabilities, has extended its applicability to the full range of macromolecular systems[15] including the analysis of hydrodynamic properties of polymeric micelles.[16] In the present study AU is demonstrated as a key characterization tool for the study of solution properties of shell cross-linked knedel nanoparticles. Additionally, analysis of solution behavior via AU clearly establishes the advantageous stability of the SCK's in comparison to their polymer micelle precursors.

Experimental Section

Sample Preparation. The SCK's were synthesized as previously described,[13] to contain a non-cross-linked polystyrene core, covalently bound to a poly(vinylpyridine) shell domain. The cross-linking of the shell was accomplished via quaternization of a portion of the 4-vinylpyridine repeat units with *p*-chloromethylstyrene, followed by polymerization of the styrenyl side chain groups. Thus, the core is hydrophobic, and the shell contains positively charged sites.

Sample solutions used for DLS measurements were prepared using previously described procedures[13] with one modification; the tetrahydrofuran (THF) present in the solutions from the synthesis of the SCK's was evaporated before DLS analysis. Solutions of SCK's and the corresponding polymer micelle precursors were analyzed immediately following THF evaporation.

Dynamic Light Scattering. Particle size distribution for SCK's in solution was determined by dynamic light scattering (DLS). The DLS instrumentation was a Brookhaven Instruments Co. (Holtsville, NY) system consisting of a model BI-200SM goniometer, a model EMI-9865 photomultiplier, and a model BI-9000AT digital correlator. Incident light was provided by a model 95-2 Ar ion laser (Lexel Corp., Palo Alto, CA) operated at 514.5 nm. All measurements were made at

† Monsanto Company.
‡ Washington University.
* Corresponding author: Tel (314) 694-4155; FAX (314) 694-6727; e-mail edward.e.remsen@monsanto.com.

10.1021/ma981951o CCC: $18.00
Published on Web 05/11/1999

21 ± 1 °C. Prior to analysis, solutions were centrifuged in a model 5414 microfuge (Brinkman Inst. Co., Westbury, NY) at 12 000*g* for 10 min to sediment dust particles.

Scattered light was collected at a fixed angle of 90°. The digital correlator was operated with 522 channels, ratio channel spacing, an initial delay time of 1 μs, a final delay time of 10 ms, and a duration time of 2 min. A photomultiplier aperture of 200 μm was used, and the incident laser intensity was adjusted to obtain a photon counting rate of at least 200 kcps. Only measurements in which measured and calculated baselines of the intensity autocorrelation function agreed to within 0.1% were used to calculate particle size. The calculation of particle size distribution and distribution averages was performed with the ISDA software package (Brookhaven Instruments Co., Holtsville, NY) which employed single-exponential fitting, cumulants analysis, and nonnegatively constrained least-squares particle size distribution analysis routines.[17] Reported particle size distribution averages are mean values of five determinations.

Electrophoretic Light Scattering. Electrophoretic mobility and zeta potential for the SCK's were determined using a Brookhaven Instruments Co. model Zeta Plus light scattering instrument. Measurements were made at 21 ± 1 °C with polymer concentrations sufficient to produce a photon counting rate of at least 500 kcps. Stock solutions of polymer were diluted with deionized water to the required polymer concentration. Reported electrophoretic mobility (μ_e) and zeta potential (ξ) are mean values of 10 analyses. Calculation of ξ from measured μ_e was provided by the built-in software supplied with the instrument. The model used in the calculation was the Smoluchowski limit ($\kappa a \gg 1$) for which the general relationship between ξ and μ_e given by[18]

$$\mu_e = (2\epsilon\xi)/(3\eta)f(\kappa a,\xi)$$

reduces to

$$\mu_e = \epsilon\xi/\eta$$

where ϵ is the dielectric constant of the medium, η is the absolute viscosity of the medium, κ is the inverse double-layer thickness, and a is the particle radius.

Analytical Ultracentrifugation. Molecular weight (M_w) and aggregation number (N_{agg}) for SCK nanoparticles were measured via sedimentation equilibrium analysis. A Beckman Instruments Co. model XL-I analytical ultracentrifuge operated with a model An50-TI, eight-hole rotor was used to ultracentrifuge aqueous solutions of SCK's to equilibrium. All measurements were made at 20 ± 0.1 °C. Rotor speeds of 5000, 8000, 12 000, and 18 000 rpm were used. Solution concentration was varied from stock solutions of several mg/mL to dilutions 1/20 the original stock solution concentration. Resulting sedimentation equilibrium patterns were recorded with both of the instrument's optics systems: a laser interferometer and an ultraviolet−visible absorbance spectrometer. The ultracentrifuge sample cell was assembled from a Epon charcoal-filled, six-channel centerpiece and matched sapphire windows. The solution volume and the cell's optical path length were 110 μL and 12 mm, respectively. The solution volume and optical path length employed corresponded to a "short" column sedimentation equilibrium experiment with a column height of approximately 2 mm. Interference scans obtained during centrifugation established that a sedimentation time of 18 h was sufficient to reach equilibrium.

Partial specific volume (v) for SCK's was determined following the method of Edelstein and Schachman.[19] This method employed H_2O and D_2O solutions of SCK's to simultaneously solve for M_w and v via comparison of the SCK's buoyant molecular weight in both solvents. Solutions of SCK in D_2O/H_2O mixtures were prepared by dilution with D_2O of stock solutions of SCK's prepared in H_2O. Solutions ranging in D_2O content from 80 to 95 vol % were sufficiently more dense than pure H_2O solutions to produce measurable changes in SCK buoyant molecular weight, thereby providing an accurate determination of v.

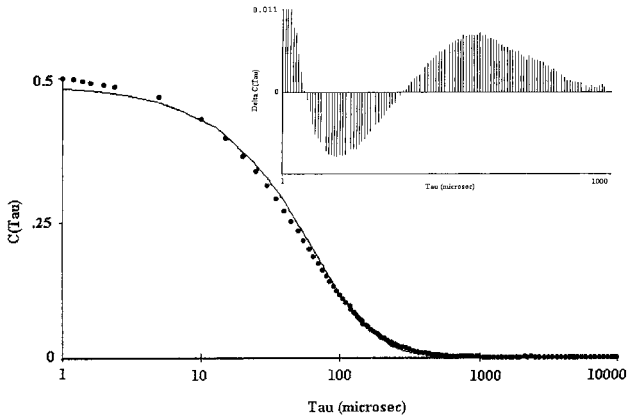

Figure 1. Single-exponential fit to intensity correlation function for SCK3 (PS:PVP = 1.9:1). Polymer solution concentration is 2.4 mg/mL in pH 7 water.

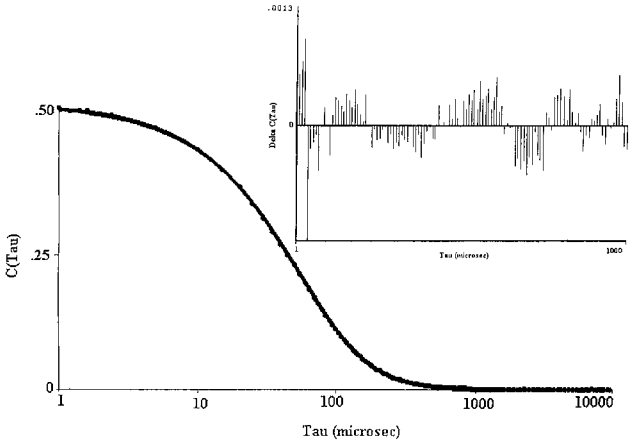

Figure 2. Double-exponential fit to intensity correlation fit for SCK3 (PS:PVP = 1.9:1). Same concentration as in Figure 1.

Calculation of molecular weight employed a built-in data analysis program that employed standard multicomponent least-squares fitting routines.[20]

Results and Discussion

SCK Hydrodynamic Diameter and Zeta Potential. A representative intensity correlation function for an SCK and an assumed single-component fit to the data are shown in Figure 1. The single-component fit to the experimental data is poor, giving nonrandom residuals (see inset in Figure 1). A two-component fit to the data, shown in Figure 2, is a more satisfactory model for the particle size distribution as judged by the randomness of the fit residuals (see inset in Figure 2). Two-component fits were required to successfully model the particle size distribution of all SCK's. Analyses of mean particle size diameters are summarized in Table 1.

For all three SCK's, the particle size averages were given by a smaller-sized major component, greater than 94 vol % in every case, and a larger-sized minor component which represented no more than 6 vol % of the particle size distribution. The mean diameter of the major component increases with increasing polystyrene block length in the SCK. Particle diameter previously determined[13] by AFM showed the same trend as summarized in Table 1. Increasing particle diameters sug-

Table 1. Summary of DLS Data

polymer	PS:PVP	D_1 (nm)	V_1 (vol %)	D_2 (nm)	V_2 (vol %)	D_m (nm)	D_{AFM} (nm)
SCK1	1:2	14 ± 1	94	53	6	16	9 ± 3
SCK2	1:1.2	21 ± 1	98	102	2	23	15 ± 2
SCK3	1.9:1	33 ± 2	96	98	4	36	27 ± 5
micelle1	1:2	35 ± 11	79	224	21	75	n.d.
micelle2	1:1.2	31 ± 7	95	113	5	35	n.d.
micelle3	1.9:1	38 ± 7	96	140	4	42	n.d.

gested an increased degree of aggregation for SCK's containing higher polystyrene block length. Molecular weight analysis via analytical ultracentrifugation (see below) supported this interpretation.

The comparison of AFM and DLS diameters indicates consistently larger diameters are found in DLS measurements. Since the DLS measurements reflect particle size in solution, while the AFM values correspond to size in the dry state, the differences between the measurements are probably due to swelling of the hydrophilic PVP shell of the SCK.[21,22] The analysis of differences between DLS and AFM diameters is complicated by the nature of the measurements provided by the techniques. Diameters measured by DLS are typically intensity-weighted values, while AFM diameters are number-average determinations. The possibility of heavier weighting in the average diameter from larger-sized species within the major component of the particle size distribution was examined by computing number-average values for the DLS data. The resulting values were only a few percent smaller than the reported D_1 values in Table 1. The polydispersity of the particle size distribution for the major component of each SCK must, therefore, be very small. This finding supports the interpretation that the larger diameters measured by DLS reflect the swelling of the hydrophilic cross-linked PVP shell of the SCK's.

A detailed analysis of the larger-sized minor component's particle size distribution was not performed. Qualitatively, this component had a larger polydispersity which could be the product of either intermolecular cross-linking of smaller-sized SCK's or the presence of larger micelle precursors previously found[13] when the stirring time employed in the synthesis of micelles was varied.

Particle distributions for solutions of un-cross-linked micelles used to prepare SCK's were also characterized by DLS. Unlike the SCK's, intensity correlation functions for the micelles were poorly modeled by two-component fits. Computed particle distribution averages, summarized in Table 1, were characterized by a major component peaking between 30 and 40 nm in diameter and a minor component with diameter in the range 100−230 nm. The major component's polydispersity was several times greater than that of its SCK counterpart. The broadness of the micelle particle size distributions accounts for the unsatisfactory fits exhibited by a two-component model.

Comparison of SCK and micelle diameters indicates a consistent decrease in diameter when micelles were cross-linked to form SCK's (see Table 1). The likely source of diameter decreases is shrinkage of the PVP shell due to cross-linking. When un-cross-linked, the quaternized PVP shell should expand to form a positively charged corona with optimum chain extension to minimize interactions between charged groups. Cross-linking contracts the PVP shell, resulting in a smaller particle. The positively charged quaternized pyridyl groups are expected to be distributed throughout the shell layer to allow for maximum charge separation, and thus some fraction of the positive charges should be located on the SCK surface.

Table 2. Summary of ELS Data

polymer	PS:PVP	[Quat][a] (mol %)	mobility (μm cm/s V)	ZP (mV)
SCK1	1:2	42	3.3 ± 0.06	44.0 ± 0.08
SCK2	1:1.2	26	2.6 ± 0.21	34.6 ± 2.6
SCK3	1.9:1	17	2.8 ± 0.21	37.6 ± 2.9
micelle1	1:2	42	3.6 ± 0.13	48.5 ± 3.1
micelle2	1:1.2	26	4.1 ± 0.13	55.0 ± 2.0
micelle3	1.9:1	17	3.3 ± 0.14	44.2 ± 1.8

[a] The mole percent of quaternized pyridyl groups determined previously[13] by elemental analysis.

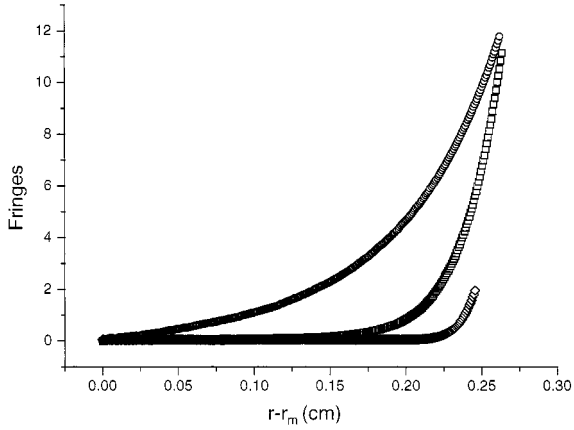

Figure 3. Representative sedimentation equilibria (fringe displacement (Fringes) versus radial distance from solution column meniscus ($r - r_m$)) for PS:PVP SCK's. Overlaid data sets corresponding to PS:PVP = 1:2 (circles), PS:PVP = 1:1.2 (squares), and PS:PVP = 1.9:1 (diamonds). All data shown were collected at 8000 rpm.

Electrophoretic mobilities and zeta potential measured by electrophoretic light scattering were positive, as summarized in Table 2, indicating a positive charge on the surfaces of the SCK's and their corresponding micelle precursors. However, the micelle mobilities and zeta potentials were generally larger than their SCK counterparts. This finding supports the expectation that a larger portion of the charge associated with the SCK may be buried below the surface of the particle and of limited mobility relative to the un-cross-linked micelle. It follows that the restriction of PVP chain conformation due to cross-linking prevents some quaternized groups from residing at the particle surface, thereby reducing the particle's electrophoretic mobility and zeta potential.

Among the set of SCK's, the polymer with the highest mole percent quaternized units exhibited the largest mobility and zeta potential, consistent with its smaller size and larger surface area, and higher content of charged units relative to the two larger SCK's.

SCK Molecular Weight and Aggregation Number. Sedimentation equilibria were generated for SCK's and micelles dispersed in water. Representative sedimentation equilibrium profiles for SCK's and micelles are shown in Figures 3 and 4, respectively. Profiles for SCK's showed a clear trend of increased sedimentation with increasing polystyrene block length and hydrodynamic diameter in the SCK (see Figure 3). A similar trend for the corresponding micelles was not observed.

Calculation of molecular weight from measured sedimentation equilibria required the determination of

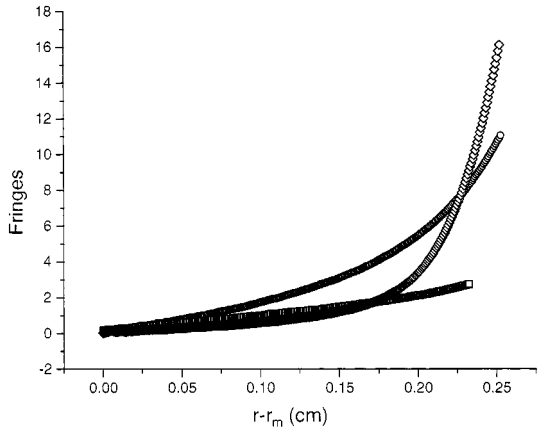

Figure 4. Representative sedimentation equilibria (fringe displacement (Fringes) versus radial distance from solution column meniscus ($r - r_m$)) for PS:PVP micelles. Overlaid data sets correspond to PS:PVP = 1:2 (circles), PS:PVP = 1:1.2 (squares), and PS:PVP = 1.9:1 (diamonds). All data shown were collected at 8000 rpm.

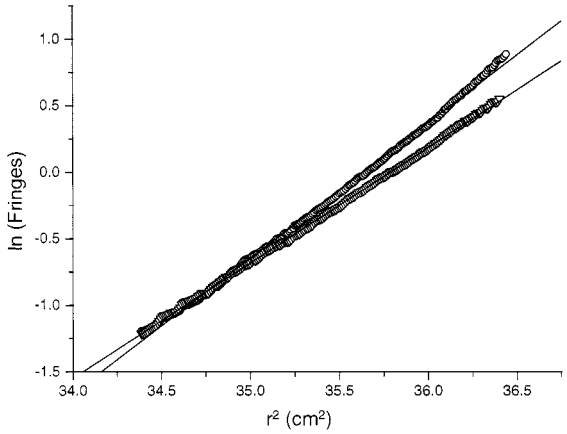

Figure 5. Representative analysis of partial specific volume (υ) from linearized sedimentation equilibrium data logarithm of fringe displacement (ln Fringes) versus radial distance squared (r^2) for SCK1 (PS:PSP = 1:2). Overlaid data sets correspond to measurements made in H_2O (circles) and a 90:10 D_2O/H_2O mixture (triangles).

partial specific volume (υ) for SCK's and micelles. Use of the traditional method of high-precision solution density measurements could not be applied because polymer concentration could not be accurately measured. This problem was overcome using the method of Edelstein and Schachman.[19] Sedimentation equilibria were measured for SCK and micelle solutions in H_2O and in H_2O/D_2O mixtures. As shown in Figure 5, sedimentation equilibria profiles for a representative SCK in the two solvents were linear when expressed as ln(fringe displacement) versus the square of radial distance. The slope of the profile for the SCK in the D_2O/H_2O (σ_D) mixture is smaller than the corresponding value measured in H_2O (σ_H). From the measurement of the two slopes, υ was determined:[19]

$$\upsilon = [1 - (\sigma_D/\sigma_H)]/[\rho_D - \rho_H(\sigma_D/\sigma_H)]$$

where ρ_D is the density of the D_2O/H_2O mixture and ρ_H is the density of H_2O.

Values of υ for SCK and micelles are summarized in Table 3. The partial specific volume of the SCK's increased as polystyrene block length increased. This result is consistent with the expected change in polymer density as a function of composition. Since the density of polystyrene is lower than the density of poly(4-vinylpyridine), υ (which is equivalent to the inverse of polymer density) should increase with decreasing polymer density.

Table 3. Summary of Sedimentation Equilibrium Data

polymer	PS:PVP	υ (mL/g)	M_w (kg/mol)	M_0 (kg/mol)	N_{agg}
SCK1	1:2	0.651	244 ± 36	20.7	12 ± 2
SCK2	1:1.2	0.716	1046 ± 78	14.7	71 ± 5
SCK3	1.9:1	0.876	6336 ± 75	14.4	439 ± 5
micelle1	1:2	0.861	279 ± 78	20.7	13 ± 4
micelle2	1:1.2	0.749	365 ± 102	14.7	24 ± 7
micelle3	1.9:1	n.d.	n.d.	14.4	n.d.

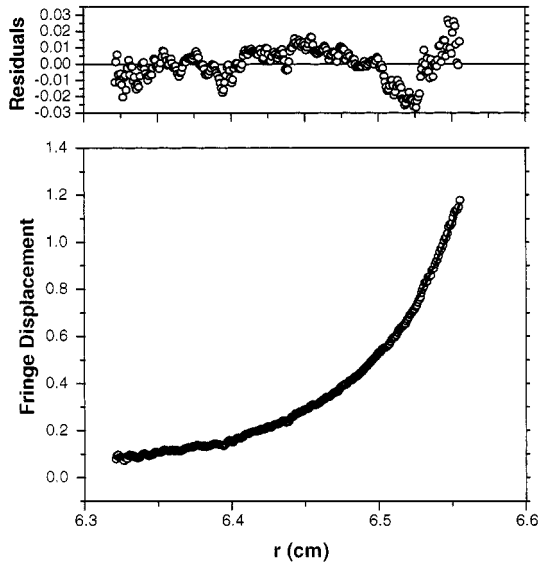

Figure 6. Representative molecular weight analysis using sedimentation equilibrium data for SCK1 (PS:PVP = 1:2). (Lower panel) Sedimentation equilibrium data (circles) and single-component least-squares fit (line). (Upper panel) Residuals of the fit. Polymer solution concentration is 0.5 mg/mL, and rotor speed is 8000 rpm.

Measurements of υ for the un-cross-linked micelles were complicated by nonlinearity in ln(fringe displacement) versus the square of radial distance. Nonlinearity suggests molecular weight heterogeneity and/or nonideal effects.[23] The structural instability for the polymer micelles, which lack the covalently cross-linked shell, may allow for changes in the micelle size and shape through the concentration gradient generated at sedimentation equilibrium. In the case of the 1.9:1 PS:PVP micelle, a single value of υ could not be obtained. Consequently, reported values are only estimates of the true values.

Using the computed values of υ, molecular weight averages for SCK's were obtained from single-component fits to sedimentation equilibrium. Representative results of this analysis are presented in Figure 6. On the basis of the apparent excellent fit and the random residuals (see upper panel in Figure 6), the SCK sedimentation profiles were well represented by single-component fits. Measurements of molecular weight were performed as a function of concentration and rotor speed. No systematic variation in molecular weight was noted with changes in concentration or rotor speed. These data suggest that SCK solutions have little or no molecular weight heterogeneity or nonideal behavior due to excluded-volume or particle−particle interactions.[23]

The finding of single components in the sedimentation equilibrium profile of SCK's would seem to contradict the finding of better modeling of DLS hydrodynamic data to two component fits. In the case of sedimentation equilibrium, the larger-sized minor component apparent in DLS data would sediment completely under the conditions used to generate sedimentation equilibria shown in Figure 6. It is, therefore, eliminated from the analysis, leaving only the smaller-sized major component. As a result, excellent single-component fits to the sedimentation equilibrium data would be expected.

The corresponding molecular weight analyses of the un-cross-linked micelles were not well modeled by single-component fits to the sedimentation equilibrium data. In addition, a strong dependence of molecular weight on micelle concentration and rotor speed was found. These data clearly indicate that the micelles are heterogeneous and exhibit nonideal effects which diminish the reliability of the molecular weight analysis. Given the heterogeneity noted earlier in the DLS data for the micelles, the indications of heterogeneity in sedimentation equilibrium data are not surprising. This is consistent with changing micelle structure during the experiment, as the block copolymer containing the shortest PS block length (relative to PVP) is expected to offer the weakest nucleation strength and to be most easily deformed. Additionally, this block copolymer (PS:PVP, 1:2) yielded micelles of the broadest size distribution (Table 1).

Molecular weights were used to determine the average aggregation number for the SCK's. As shown in Table 3, the trend in aggregation number paralleled the previous noted trends in hydrodynamic diameter and molecular weight; i.e., as the polystyrene block length in SCK increases, its average aggregation number also increases.

SCK Hydrodynamic Shell Thickness. Using PS:PVP copolymer molecular weight, SCK degree of aggregation, hydrodynamic diameters, and polystyrene density, estimates of SCK hydrodynamic shell thickness were calculated. Formation of the 1:2 SCK (SCK1) with a measured copolymer molecular weight of 20 700 g/mol and mean degree of aggregation of 12 copolymer chains yielded an equivalent spherical polystyrene core radius of 3.1 nm, assuming a density corresponding to a nominal value of 1.053 g/mL for amorphous polystyrene.[24] The difference between the hydrodynamic radius measured by DLS and the polystyrene core radius gives an estimated hydrodynamic shell thickness of 3.9 nm. Calculation of the polystyrene core radius for the 1:1.2 SCK (SCK2) and the 1.9:1 SCK (SCK3) gave values of 5.6 and 11.4 nm, respectively. Estimated hydrodynamic shell thicknesses for SCK2 and SCK3 were calculated as the difference between the DLS hydrodynamic radius and the polystyrene core radius, yielding values of 4.9 and 5.1 nm, respectively.

Conclusions

The characterization of solution properties for PS:PVP SCK's and their micelle precursor was readily accomplished using a combination of techniques. Dynamic light scattering determinations of hydrodynamic diameter demonstrated that particle diameter increases with increasing polystyrene content in the PS:PVP block copolymer used to prepare the micelle precursor to an SCK. In a similar manner, analytical ultracentrifugation (AU) molecular weight analysis showed that SCK molecular weight and the corresponding degree of aggregation also increase with increasing polystyrene content. AU also revealed the presence of strong nonideal effects in the solution properties of micelle precursors. Nonideal behavior was attributable to an inherently less stable structure of the micelle which is subject to deformation and distortion under ultracentrifugation. Finally, multitechnique characterization of SCK's provided sufficient data to estimate hydrodynamic shell thickness. As polystyrene content increased in the SCK, the core radius increases significantly and the shell thickness also increases, paralleling observed trends in SCK hydrodynamic diameter, molecular weight, and degree of aggregation.

Acknowledgment. The authors thank the Brookhaven Instrument Co. for the use of an electrophoretic light scattering instrument. Funding for the preparation of the SCK's was provided by the National Science Foundation NYI Program (DMR-9458025).

References and Notes

(1) Kiser, P. F.; Wilson, G.; Needham, D. *Nature* **1998**, *394*, 459.
(2) Stupp, S. I.; Braun, P. V. *Science* **1997**, *277*, 1242.
(3) Nelson, J. C.; Saven, J. G.; Moore, J. S.; Wolynes, P. G. *Science* **1997**, *277*, 1793.
(4) Benyus, J. M. *Biomimicry: Innovation Inspired by Nature*; William Morrow and Co., Inc.: New York, 1997.
(5) Nanostructured Materials, special issue of *Chem. Mater.* **1996**, *8* (8).
(6) Martin, C. *Science* **1994**, *266*, 1961.
(7) Xia, Y.; Kim, E.; Zhao, X. M.; Rogers, J. A.; Prentiss, M.; Whitesides, G. *Science* **1996**, *273*, 347.
(8) *Advances in Dendritic Molecules*; Newkome, G. R., Ed.; JAI Press: Greenwich, CT, 1994, 1995; Vols. 1 and 2.
(9) Evans, E.; Bowman, H.; Leung, A.; Needham, D.; Tirrell, D. *Science* **1996**, *273*, 933.
(10) Ishizu, K.; Fukutomi, T. *J. Polym. Sci., Part C: Polym. Lett.* **1988**, *26*, 281.
(11) Zhang, L.; Eisenberg, A. *Science* **1995**, *268*, 1728.
(12) Percec, V.; Johansson, G.; Ungar, G.; Zhou, J. *J. Am. Chem. Soc.* **1996**, *118*, 9855.
(13) Thurmond, K. B. II; Kowalewski, T.; Wooley, K. L. *J. Am. Chem. Soc.* **1997**, *119*, 6656.
(14) Schachman, H. K. *Ultracentrifugation in Biochemistry;* Academic Press: New York, 1959.
(15) Schachman, H. K. *Nature* **1989**, *341*, 259.
(16) Morgan, P. J.; Harding, S. E.; Petrak, K. *Macromolecules* **1990**, *23*, 4461.
(17) Stock, R. S.; Ray, W. *J. Polym. Sci., Polym. Phys.* **1985**, *23*, 1393.
(18) von Smoluchowski, M. *Z. Phys. Chem.* **1918**, *92*, 129.
(19) Edelstein, S. J.; Schachman, H. K. *J. Biol. Chem.* **1967**, *242*, 306.
(20) Johnson, M. L.; Correia, J. J.; Yphantis, D. A.; Halvorson, H. R. *Biophys. J.* **1981**, *36*, 575.
(21) Huang, H.; Wooley, K. L.; Remsen, E. E. *Chem. Commun.* **1998**, *13*, 1415.
(22) Huang, H.; Kowalewski, T.; Remsen, E. E.; Gertzmann; R.; Wooley, K. L. *J. Am. Chem. Soc.* **1997**, *119*, 11653.
(23) Munk, P.; Halbrook, M. E. *Macromolecules* **1976**, *9*, 568.
(24) *Polymer Handbook*, 2nd ed; Brandrup, J., Immergut, E. H., Eds.; John Wiley & Sons: New York; Chapter V, p V-59.

MA981951O